Localization of cyanobacterial photosystem II donor-side subunits by electron microscopy and the supramolecular organization of photosystem II in the thylakoid membrane

Kuhl, Helena; Rögner, Matthias; Breemen, Jan F.L. van; Boekema, Egbert J.

Published in:
European Journal of Biochemistry

Publication date:
1999

Eur. J. Biochem. **266**, 453–459 (1999) © FEBS 1999

Localization of cyanobacterial photosystem II donor-side subunits by electron microscopy and the supramolecular organization of photosystem II in the thylakoid membrane

Helena Kuhl[1], Matthias Rögner[1], Jan F. L. van Breemen[2] and Egbert J. Boekema[2]

[1]*Lehrstuhl für Biochemie der Pflanzen, Fakultät für Biologie, Ruhr-Universität Bochum, Germany;* [2]*Groningen Biomolecular Sciences and Biotechnology Institute, University of Groningen, the Netherlands*

A large set of electron microscopy projections of photosystem II (PSII) dimers isolated from the cyanobacterium *Synechococcus elongatus* was characterized by single particle image analysis. In addition to previously published maps at lower resolution [Boekema, E.J., Hankamer, B., Bald, D., Kruip, J., Nield, J., Boonstra, A.F., Barber, J. & Rögner, M. (1995) *Proc. Natl Acad. Sci. USA* **92**, 175–179], the new side-view projections show densities of all three lumenal extrinsic proteins, i.e. the 33-kDa, 12-kDa and the cytochrome *c*-550 subunit encoded by *psbO*, *psbU* and *psbV*, respectively. Analysis of the size and shape of the top-view projections revealed a small number of photosystem II particles of about double the size of the usual dimers. Size and quantity of these 'double dimers' correlates with a small fraction of 1000-kDa particles found with HPLC-size-exclusion chromatographic analysis. Because many cyanobacteria contain dimeric photosystem II complexes arranged in rows within the membrane, the double dimers can be considered as the breakdown fragments of these rows. Their analysis enabled the detection of the arrangement of photosystem II within the rows, in which the dimers interact with other dimers mostly with their tips, leaving a rather open center at the interfaces of two dimers. The dimers have a repeating distance of only 11.7 nm. As a consequence, the phycobilisomes, located on top of PSII and functioning in light-harvesting, must be closely packed or almost touch each other, in a manner similar to a recently suggested model [Bald, D., Kruip, J. & Rögner, M. (1996) *Photosynthesis Res.* **49**, 103–118].

Keywords: photosystem II; thylakoid membrane; extrinsic subunits; electron microscopy.

Photosystem II (PSII) has a highly complicated structure due to its large number of different subunits [1]. Nevertheless, during the last 5 years the resolution of the PSII structure has been steadily improved. Recently, an 0.8-nm structure of the PSII CP47-reaction center obtained by electron microscopy of two-dimensional crystals has been published [2]. This structure shows the position of 23 transmembrane α-helices, 16 of which could be assigned to the D1 and D2 subunits and the largest proximal antenna subunit CP47. Together with the other proximal antenna subunit, CP43, three different extrinsic subunits and several low molecular subunits they form the core complex, the smallest particle still capable to evolve oxygen. It is now well established that *in vivo* the PSII core particle exists as a dimer [1,3]. However, the crystal structure lacks information about the three lumenal extrinsic subunits of the oxygen evolving complex, because they are lost during isolation. While PSII from green plants contains three such proteins, the so-called 33, 23 and 17-kDa proteins (reviewed in [4]), the cyanobacterial PSII core complex lacks the 23- and 17-kDa protein and, instead, contains the cytochrome (Cyt) *c*-550 and the 12-kDa subunit [5]. Functional studies indicate that Cyt *c*-550 plays a substantial role in maintaining the stability and function of the manganese cluster, whereas the 12-kDa protein plays primarily a regulatory role in maintaining normal S-state transitions [6–9]. Double deletion mutants lacking Cyt *c*-550 and the 12-kDa protein still grow photoautotrophically [8], while double deletion mutants of Cyt *c*-550 and the 33-kDa protein results in loss of photoautotrophic growth and show almost no oxygen evolution activity [6,7].

Analysis of projections from dimeric PSII supercomplexes isolated from green plants by electron microscopy has indicated the presence of two 33-kDa subunits and two 23-kDa subunits with respective center-to-center distances of 6.3 nm and 8.8 nm [10]. The side-view projections of these supercomplexes have been particularly useful in these studies, showing that the 23-kDa protein was not always present, while the 17-kDa subunit was absent. In cyanobacterial PSII the position of the two smallest extrinsic proteins, Cyt *c*-550 and the 12-kDa subunit, has not yet been investigated due to the fact that these subunits have been lost in the particles studied up to now [11]. Concerning the overall structure, PSII core complexes of cyanobacteria and green plants are structurally quite similar [11], but they have a very different peripheral antenna system. Green plant core complexes are associated with numerous copies of six different membrane-bound light-harvesting proteins [12] forming supercomplexes and megacomplexes [11,13]. Cyanobacteria do not have a membrane-integrated antenna system; instead they have a very large water-soluble light-harvesting system, the phycobilisome [14]. These phycobilisomes are attached on rows of dimeric PSII particles, as has been demonstrated by freeze-fractured membrane specimens [15]. Based on this finding, and the size and shape of the

Correspondence to E. J. Boekema, Groningen Biomolecular Sciences and Biotechnology Institute, University of Groningen, Nijenborgh 4, 9747 AG Groningen, the Netherlands. E-mail: boekema@chem.rug.nl

Abbreviations: Cyt, cytochrome; D1 and D2, products of the *psbA* and *psbD* genes, respectively; PSII, photosystem II.

(Received 30 June 1999, revised 20 September 1999, accepted 21 September 1999)

isolated cyanobacterial PSII dimer [11], a model for the attachment of the phycobilisomes to these rows in cyanobacteria was proposed [16]. To verify this model, it would be useful to determine the exact position of the PSII dimers within these rows by electron microscopy. Two approaches could be followed: partial solubilization of the membranes, as was carried out with the stacked thylakoids from spinach [17], and a search for the presence of larger (row-like) aggregates in negatively stained specimens; and a search in purified PSII samples for complexes larger than the usual dimers. After an initial effort with partially solubilized membranes, the second approach proved to be successful.

In this study, we present the re-investigated PSII core structure based on a large (several thousands of projections) data set. The analysis showed that among the top-view projections, both the previously characterized dimeric PSII particles [11] and additional double dimers of PSII are present. The features of this projection reveal the position of the two dimers quite well, from which the precise orientation of the PSII dimers in the row-like aggregates can be deduced. The analysis of the side-view projections also showed new features. Close to the protrusions of the 33-kDa extrinsic subunits, two sets of two other densities are present, which can be assigned to the Cyt *c*-550 and the 12-kDa subunit, constituting, together with the 33-kDa subunit, the oxygen-evolving complex in cyanobacterial PSII [5].

MATERIALS AND METHODS

Isolation and biochemical characterization of PSII complexes

PSII core complexes from *Synechococcus elongatus* were prepared as in [11] with some modifications. Essentially, after extraction of the proteins from the thylakoid membrane the sucrose gradient was omitted and pure PSII complexes were obtained by two HPLC column steps. Oxygen evolution activity using 2 mM dichloro-*p*-benzoquinone as electron acceptor was 5000–6000 μmol $O_2 \cdot h^{-1} \cdot$mg chlorophyll^{-1}. The core particles were frozen in buffer containing 20 mM Mes, pH 6.5, 10 mM $CaCl_2$, 10 mM $MgCl_2$, 0.5 M mannitol and 0.03% β-dodecyl maltoside and stored at −70 °C prior to use. More details of this preparation are provided in [18]. Size-exclusion chromatography was performed on a Waters system consisting of a photodiode array detector 996, pump 515 and an injector (Rheodyne) with a TSKgel 4000 SWXL column (TosoHaas) using a buffer of 20 mM Mes, pH 6.5, 30 mM $CaCl_2$, 10 mM $MgCl_2$, 0.5 M mannitol and 0.03% β-dodecyl maltoside at a flow rate of 0.5 mL$\cdot$min^{-1} [5].

Electron microscopy and image analysis

Transmission electron microscopy was performed with a Philips CM10 electron microscope using 80 kV at 52 000× magnification. Negatively stained specimens were prepared on carbon-coated copper grids. Part of the grids were glow-discharged before preparing electron microscopy specimens to enhance the absorption of PSII particles with their hydrophilic parts, which results in predomination of top-view projections. Other grids were used without this treatment and yielded electron microscopy specimens with mainly side-view projections. Micrographs were digitized with a Kodak Eikonix Model 1412 CCD camera with a step size of 25 μm, corresponding to a pixel size of 0.485 nm at the specimen level. From 99 images, close to 5000 well-preserved top- and side-view projections were extracted for image analysis with IMAGIC software [19]. The 3640 selected top-view projections and 964 side-view projections were aligned, treated by multivariate statistical analysis and classified, as described previously [11,19].

RESULTS AND DISCUSSION

Analysis of top-view projections of PSII dimers

Isolated and purified PSII dimers were characterized by size-exclusion chromatography (Fig. 1) and SDS/PAGE (Fig. 2). While about 95% of the preparation showed a homogenous peak at the position where dimeric PSII is expected to elute, about 5% of the sample eluted at about 1000 kDa, indicating the existence of particles with the double mass of PSII dimers (referred to as 'double dimers', Fig. 1). Absorbance spectra of both peaks recorded by an online photo diode array detector show no differences. Such typical dimeric PSII preparations were also characterized by electron microscopy of negatively stained images followed by image analysis. The images clearly

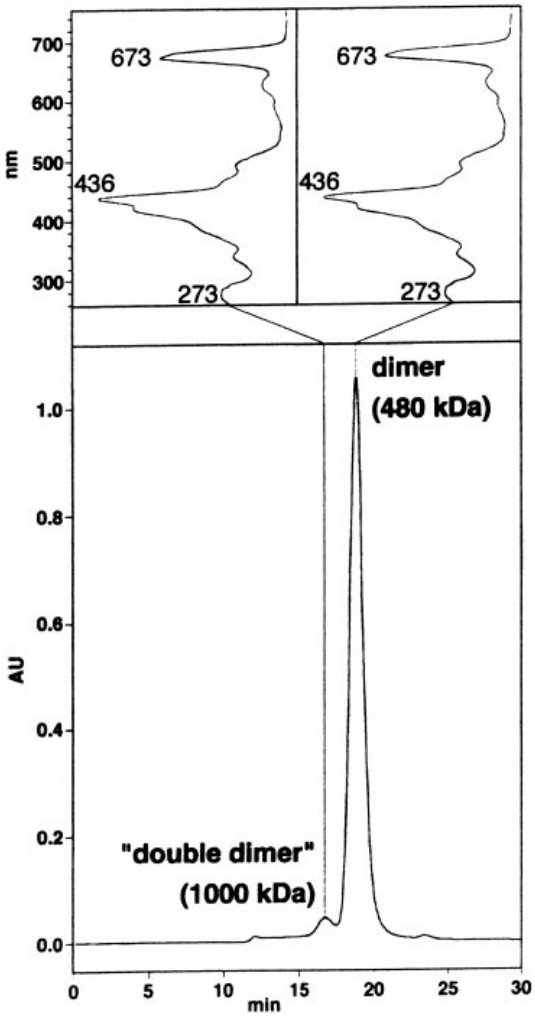

Fig. 1. Elution profile of purified PSII. Results from size-exclusion chromatography (TSK 4000 SW_{XL} column) and absorption spectrum of the two main peaks. In the lower part of the figure, the large peak indicates PSII dimers of approximate 480 kDa running at 19 min, while the small peak on the left indicates a particle of about 1000 kDa; according to their absorbance spectra recorded online by a diode array detector (Waters) (upper part), both fractions contain PSII complexes. AU, arbitrary units.

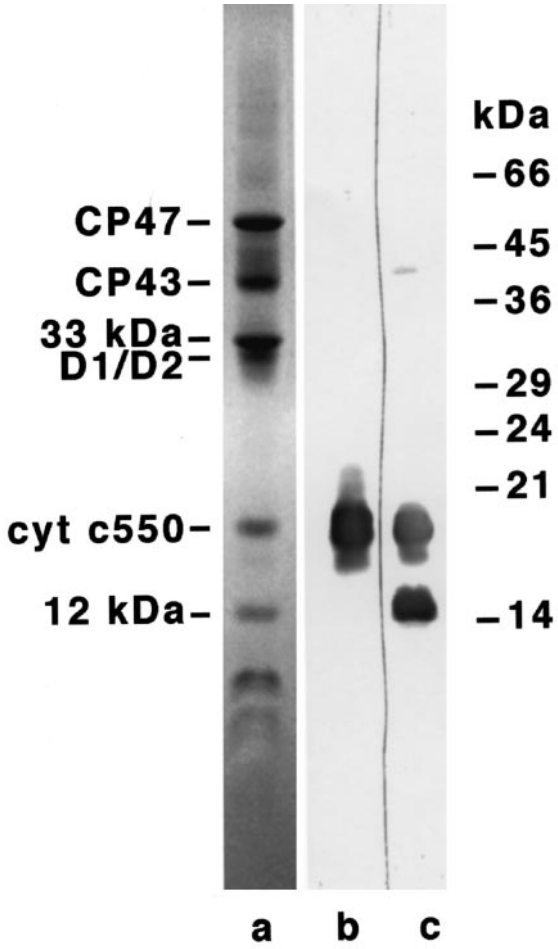

Fig. 2. SDS/PAGE of purified PSII. Subunits were separated on a 12–22% SDS-gradient gel with a Tris concentration of 3 M. Lane a, purified PSII dimer, Coomassie stained. Lanes b and c, immunoblot analysis of purified PSII dimer with antibodies against Cyt *c*-550 (lane b) and the 12-kDa protein (lane c), respectively. The anti-12 kDa antibody also cross-reacts with Cyt *c*-550 due to a small amount of Cyt *c*-550 contaminating the 12-kDa protein antigen preparation used to prepare the antibodies.

show that the preparation contains monodispersely solubilized particles with the shape and size of dimeric PSII, which is almost free from contaminants (Fig. 3). For a more precise characterization by image analysis, a large data set was extracted from 99 images. During the particle selection step we noticed a few trimeric top-views of PS I molecules, a few tetrameric views of Rubisco and also some side-views of phycobilisome fragments, recognizable by a narrow parallel striation pattern. In comparison to the large number of well-preserved PSII dimers it can be concluded that these contaminants occur with a frequency of 0.1% or less indicating the high purity of this preparation. Another characteristic component of this sample with approximately the double size of a dimer will be described below.

After three cycles of multi-reference alignment, multivariate statistical analysis and classification, the top-view data set was decomposed in a final step into eight classes: the eight class-sums are presented in Fig. 4. Although they all appear rather similar, a deviation from perfect twofold rotational symmetry is clear in five out the eight classes (Fig. 4A,C,D,F,H). A similar partial deviation from a rotational symmetry has been reported for trimeric PS I [20]. It was interpreted to be due to tilting of molecules, originating from short-range roughness of the carbon support film. The tilting effect is only strong in the direction of the short axis through the molecule and can be seen as a smearing-out of density on one side of the molecular projections (the lower side of Figs 4A,D and 3H and the upper side of Fig. 4C,F, particles; see also [21] for a similar case). It is likely that the variation in the projections is also influenced by a variation in the amount of binding of the extrinsic subunits, but this variation is obviously much smaller than in the side-views (see below) and difficult to quantify from the classification. To obtain the highest resolution in the untilted view, projections of the three classes with the strongest twofold rotational symmetry (Fig. 4B,E,G; 1054 views) were re-analyzed; the sum of the best 225 images is presented in Fig. 6A). It shows a slightly better resolution (about 2 nm, as determined by the Fourier-ring correlation method [22]) than obtained previously [11]. Especially the two most stain-excluding densities, assigned to the 33-kDa extrinsic protein and CP47, which are separated by about 2.3 nm in spinach PSII supercomplexes (densities A and B in Fig. 6D, top, and in [10]) are now also becoming separated in the core top-views (Fig. 6A). These masses were not separately resolved in either spinach or cyanobacterial PSII core complexes before [11].

Analysis of side-view projections of PSII dimers and location of the extrinsic subunits

A total of 964 side-view projections were analyzed (Fig. 5). An initial classification of the data set showed that some of the variation among the side-views corresponds with changes in the overall length in projection. A minority of views, represented by the class-sums of Fig. 5F,G, was substantially shorter than

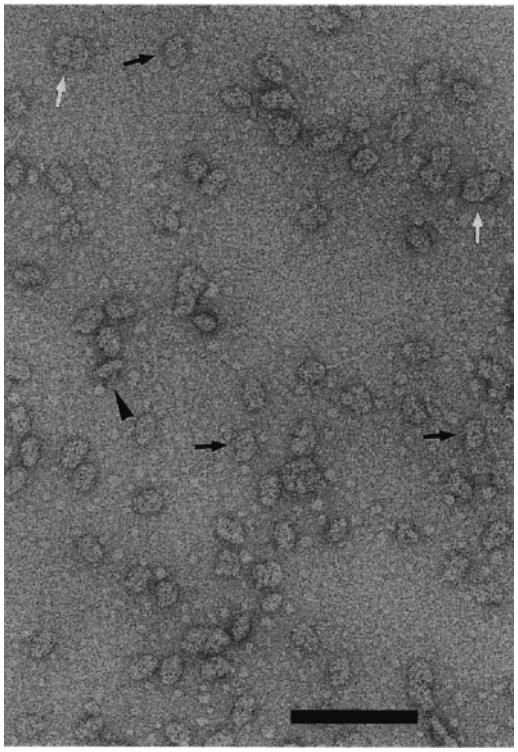

Fig. 3. Electron micrograph of isolated PSII core complexes. Samples were negatively stained with 2% uranyl acetate. Black arrows point to top-view projections of dimers, white arrows to double dimers and a black arrowhead to a dimer in side-view position. The scale bar is 100 nm.

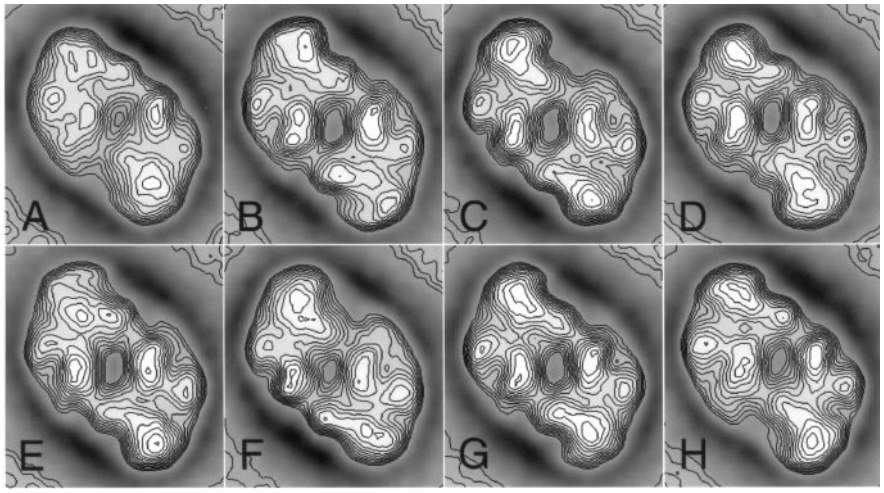

Fig. 4. Results of multivariate statistical analysis and classification of top-view projections. A data set of 3540 PSII core dimers was decomposed into eight classes, with members of projections between 333 and 401. The contoured class-sum images are presented as facing from the p-side of the thylakoid membrane, which is equivalent to the lumenal side in green plants.

expected. They may all represent projections of particles that are not attached with the longest axis parallel to the carbon support film and were omitted in the final classification, which is presented in Fig. 5A–E. These classes show a substantial variation in the appearance of the protrusions. The most abundant projection type (Fig. 5A), is rather similar to the predominant view found before [11]. It shows two separated protrusions, symmetrically located with respect to the center of the complex. In other classes, additional protrusions are present aside from the two central protrusions (Fig. 5B–D), with the inner protrusions being incomplete in some of the projections (Fig. 5D). Notably, this is the first time that the outer protrusions are observed in cyanobacterial PSII images [11]; for details of the previous analysis, see [23]. In the projection with the most complete outer protrusions (Fig. 5C) the PSII particle has an overall height of 9.5 nm. This is identical to PSII from spinach in which, instead of the Cyt *c*-550, the extrinsic 23-kDa protein is attached [10]. In cyanobacteria, it is very likely from functional and cross-linking studies that the outer protrusions consist of the Cyt *c*-550 and the 12-kDa subunits, while the inner protrusions consist of the 33-kDa subunits [24,25]. In fact, our images are in agreement with these studies, if we assume that the lower part of the outer protruding mass is formed by the Cyt *c*-550 subunit and the upper part by the 12-kDa subunit, as proposed [25]. This is especially supported by the observation that the 12-kDa protein does not bind to PSII at all unless the 33-kDa protein or Cyt *c*-550 is present [25]. The presence of all these small subunits in our preparation can be seen from SDS/PAGE and immunoblotting (Fig. 2) and, in case of Cyt *c*-550, by heme staining (results not shown). Our modified model as shown in Fig. 6C would explain the following features: (a) the image of Fig. 5A shows average particles with only the two central 33-kDa proteins present, while the image of Fig. 5C represents particles with all three extrinsic proteins present in two copies; (b) the image of Fig. 5D with the inner protrusions being much more reduced than the outer ones, is consistent with the observation that the Cyt *c*-550 subunit can bind to PSII almost independently from the 33-kDa subunit [25]; (c) the difference between the images of Fig. 5B,C could be explained by the absence of the 12-kDa protein in Fig. 5B – this is consistent with the observation that the 12-kDa protein can only bind to PSII in the presence of both the 33-kDa protein and Cyt *c*-550. The observation that the 12-kDa subunit requires the presence both other extrinsic subunits suggests a localization between the Cyt *c*-550 and the 33-kDa subunit; this is also reflected in the image of Fig. 5C, where no clear spacing between the inner and outer protrusions is visible anymore, in contrast to Fig. 5B where the 12-kDa subunit is possibly lacking.

Knowing these distances, it is tempting to try to assign the extrinsic subunits in the top view projection as well. Figure 6A,B shows averaged top- and side-views in compatible positions, while Fig. 6C tries to combine them in a model. For comparison, also the top view of the PSII-supercomplex from spinach is shown [10], which yielded 5 densities in the core part (marked A–E in Fig. 6D). In the top views of the cyanobacterial PSII core complex, the same densities are visible (Fig. 6A,C). Figure 5B,C indicates that in the side-view

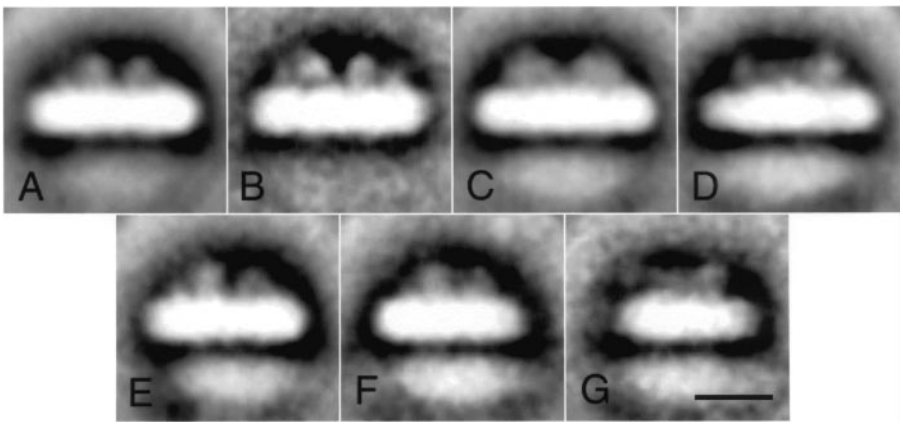

Fig. 5. Analysis of side-view projections of dimeric PSII core complexes. (A–E) Five final class-sums of last classification, with 198, 143, 100, 39 and 59 images, respectively; (F,G) two class-sums with 38 and 79 images from an initial classification showing a smaller projected length. The scale bar is 10 nm.

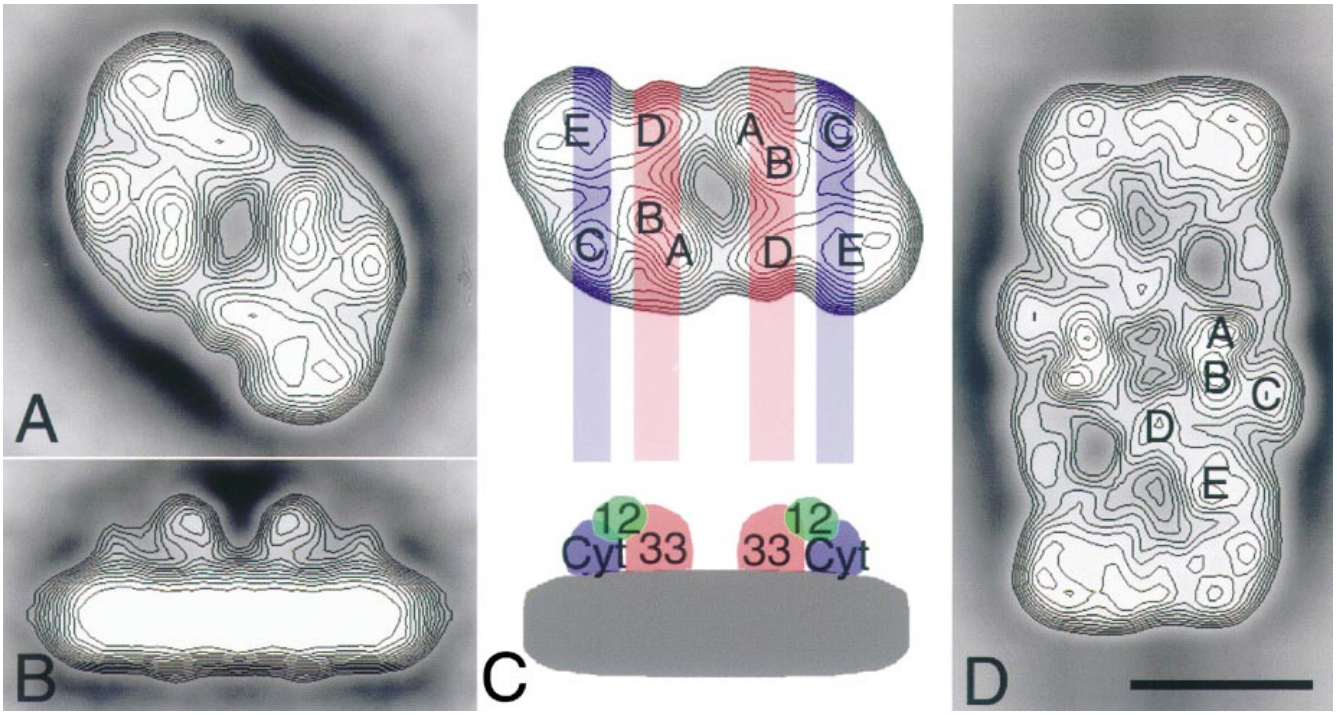

Fig. 6. Position of the extrinsic subunits of PSII. (A) Contoured version of the twofold symmetrized final sum of the best 225 projections from Fig. 3; (B) contoured averaged side view of Fig. 4B, with imposed mirror-symmetry; (C) averaged top view with letters marking areas of highest protein density and regions for the localization of Cyt *c*-550 and 33 kDa-subunits marked by purple and red stripes, respectively (top); suggested model for the localization of the extrinsic proteins Cyt *c*-550 (Cyt), 12-kDa protein (12) and 33-kDa subunit (33) (bottom); (D) average projection of the PSII supercomplex from spinach with the five densities forming the core part monomer indicated with A–E (see [10]). The scale bar is 10 nm.

projection the Cyt *c*-550 subunit protrusions are at a distance of 14 nm. In the top view projection, these two protrusions would be along two lines in a direction vertical to the long axis of the dimer and spaced by 14 nm (Fig. 6C). These lines intercept the densities C and E (Fig. 6C, top), which are consequently the potential candidates for the Cyt *c*-550 position. As the density C is close to B, the site of the 33-kDa extrinsic subunit [10], this density is very likely occupied by the Cyt *c*-550 subunit. Considering density C as the likely position for Cyt *c*-550 the spacing between the centers of mass of the 33-kDa protein, B, and the Cyt *c*-550 protein, C, is then 3.7 nm. However, considering their actual masses of 29 kDa and 17 kDa, the two proteins would be separated by only about 0.5 nm. In contrast, the distance between the centers of mass of densities E and B is 6.5 nm. As the Cyt *c*-550 subunit crosslinks directly with the 33-kDa protein with the zero-length crosslinker 1-ethyl-3-(3-dimethylaminopropyl)-carbodiimide [24], these proteins must have close contact, which leads to the assignment of the Cyt *c*-550 subunit on density C.

Although unlikely, our data do not, however, exclude that Cyt *c*-550 could be located on density E (and/or D), as we see the extrinsic proteins only in one specific side-view orientation.

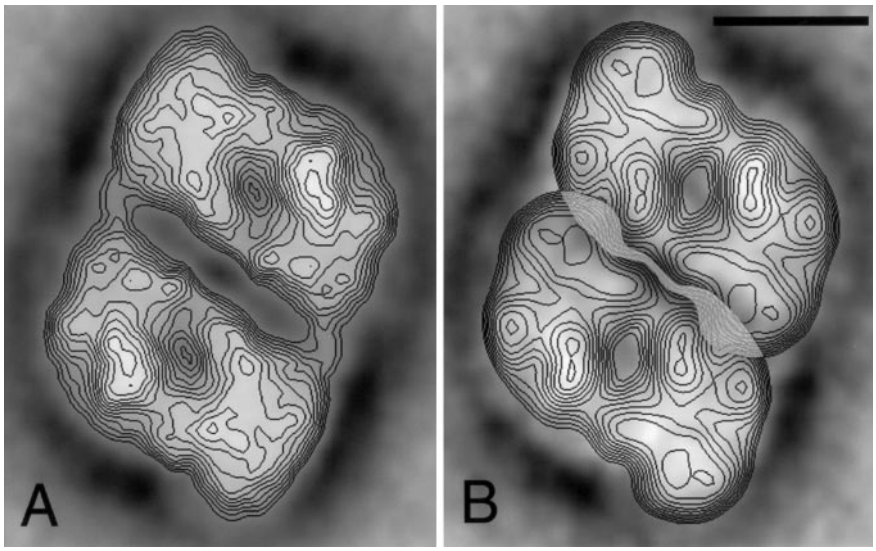

Fig. 7. Positioning of single dimers into double dimers of PSII. (A) Sum of 69 aligned projections of isolated double dimers with twofold symmetry imposed after analysis; (B) sum of (A) (without contours) on which the contours of the image of Fig. 6A were superimposed after fitting of the positions. The fitted dimers overlap with their detergent boundary layer, as indicated by the grey overlayer, especially at the periphery of the interface. Assuming that the real PSII dimensions without detergent are at least 1 nm smaller [30], it follows that the center of the double dimer is rather open and that the dimers interact mostly with their tips. The scale bar is 10 nm.

Interestingly, in green plant PSII supercomplexes, where the core part was visualized under a different angle from aside, it was very obvious that the 23-kDa subunit (the structural green-plant analog to the Cyt *c*-550 subunit) was positioned on density D [10] and that a positioning on C was difficult to (dis)prove due to the overlap with the neighboring 33-kDa protein, although there was a clear difference in the top views [10]. The most likely explanation of the finding of two clearly different positions for the 23-kDa and the Cyt *c*-550 subunit, respectively, would be that two such proteins exist in one native monomeric core complex. This could imply that two copies of the other two extrinsic proteins are present as well. This is supported by strong biochemical evidence for a second 33-kDa extrinsic subunit per monomer [26–28]. With the present data, a clear assignment of two potential copies of the 33-kDa subunits is not yet possible, i.e. further experiments with PSII-particles containing defined numbers of extrinsic subunits are necessary.

Analysis of top-view projections of double dimers

Besides the PSII dimer described above, another class of particles was observed with a frequency of about 1% relative to the PSII dimers. Image analysis revealed that this larger particle consisted of two associated PSII dimers, which are shown as a sum of 69 projections in Fig. 7A. The identification of these 'double dimers' as two associated PSII core dimers is strongly supported by the elution profile obtained by size-exclusion chromatography (Fig. 1) in combination with absorption spectra. Despite the noisy appearance due to the limited number of added projections, the two halves of the double dimer are very similar to the single dimer, as indicated by a cross-correlation coefficient of about 0.7 (a value of 1.0 indicates identity [29]). Therefore the sum of these double dimers is presented with a twofold symmetry imposed. Due to stain accumulation in the center, the similarity between double dimers and single dimers is, however, lower at the interface. For a closer comparison, we fitted the image of the dimer of Fig. 6A in the two halves of the double dimer of Fig. 7A. The fit, Fig. 7B, can only be carried out if the two dimers overlap about 0.6 nm in the center and maximally 2.2 nm at the periphery (Fig. 7B). The overlap in the double dimer can easily be explained by the detergent boundary layer which surrounds the isolated single dimers [30], but is lacking in the hydrophobic contact area of the double dimers. This strongly supports the presence of such double dimers in the thylakoid membrane.

Although formation of double dimers by aggregation of single dimers after isolation cannot be excluded, the probability of this is low as it would require a substantial detergent rearrangement. In parallel, we also examined partially solubilized membranes, as was carried out previously with green plant thylakoid membranes [17]. We found a few double dimers projections in the fragmented membranes (not shown), indicating that they do indeed exist *in vivo*. The number was, however, much lower than in the case of spinach, where the PSII containing-membranes are stacked and (almost) free of PS I, ATPase and other proteins involved in the primary and secondary reactions of photosynthesis. In conclusion, both types of experiments yield only one type of double dimers, indicating a specific interaction of the involved dimers and possibly also within larger units, such as the arrangement in rows, which are known to occur *in vivo* (see below). Judging from Fig. 7A, the interaction between the dimers within the rows is merely between the tips, thus leaving a some open space in the centers, possibly filled with lipids *in vivo*. From this image, a repeating distance of PSII dimers in the row of 11.7 nm can be deduced and an angle between the long axis of the dimer and the rows of about 73°.

Implications for PSII organization and phycobilisome association

A row-like organization of dimeric PSII complexes in cyanobacterial thylakoid membranes was visualized by electron microscopy using freeze-fracture specimens. Repeating distances of 10–12 nm [15] and 14 nm [31] for PSII dimers within the rows were found for two different specimens. Based on these data, a model for the positioning of the dimers and phycobilisomes was proposed [16]. This model should now be slightly modified; according to the new data, the dimers in the rows are 2 nm closer and they also need to be shifted 4 nm laterally. Although the exact arrangement of the phycobilisomes on the PSII rows remains to be experimentally established, some images of partly purified PSII–phycobilisome preparations indicate that in the direction vertical to the rows, the PSII molecules are somewhat asymmetrically arranged underneath the phycobilisomes [32]. On the other hand, it ihas now been shown that both the core part of the phycobilisome and the PSII core complex have a twofold symmetry [1,33]. In other words, the parts of both systems that are facing each other are arranged in an antiparallel way, thus strongly suggesting a symmetrical attachment of the phycobilisome on top of the PSII complex, as was already proposed in the previous model [16]. The most relevant consequence of the new data is the closer packing of the phycobilisomes as the distance between the dimers is only 11.7 nm. Thus the phycobilisomes in *Synechococcus elongatus* almost touch each other. The fact that the phycobilisomes are so close, should enable some excitation energy transfer between neighboring phycobilisomes, thus creating highly efficient 'pipelines' [34], composed of phycobilisome core complexes on top of the dimeric PSII complexes.

ACKNOWLEDGEMENTS

We thank Dr W. Keegstra for his help with image processing, Mr K. Gilissen for photography, Marion Bünker for excellent technical assistance and Prof. A. Brisson for stimulating discussions. The antibodies were kindly provided by Dr J.-R. Shen, RIKEN Harima Institute, Japan. The financial support of the DFG (SFB 480, MR and Graduiertenkolleg, HK) is gratefully acknowledged.

REFERENCES

1. Hankamer, B., Barber, J. & Boekema, E.J. (1997) Structure and membrane organization of photosystem II in green plants. *Annu. Rev. Plant Physiol. Plant Mol. Biol.* **48**, 641–671.
2. Rhee, K.-H., Morris, E.P., Barber, J. & Kühlbrandt, W. (1998) Three-dimensional structure of the plant photosystem II reaction centre at 8 Å resolution. *Nature* **396**, 283–286.
3. Rögner, M., Dekker, J.P., Boekema, E.J. & Witt, H.T. (1987) Size, shape and mass of the oxygen-evolving photosystem II complex from the thermophilic cyanobacterium *Synechococcus* sp. *FEBS Lett.* **219**, 207–211.
4. Seidler, A. (1996) The extrinsic polypeptides of photosystem II. *Biochim. Biophys. Acta* **1277**, 35–60.
5. Shen, J.-R., Ikeuchi, M. & Inoue, I. (1992) Stoichiometric association of extrinsic cytochrome c550 and 12 kDa protein with a highly purified oxygen-evolving photosystem II core complex form *Synechococcus vulcanus*. *FEBS Lett.* **301**, 145–149.

6. Shen, J.-R., Burnap, R.L. & Inoue, Y. (1995) An independent role of cytochrome *c*-550 in cyanobacterial photosystem II as revealed by double-deletion mutagenesis of the *psb*O and *psb*V genes in *Synechocystis* sp. PCC 6803. *Biochemistry* **34**, 12661–12668.
7. Shen, J.-R., Vermaas, W. & Inoue, Y. (1995) The role of cytochrome *c*-550 as studied through reverse genetics and mutant characterization in *Synechocystis* sp. PCC 6803. *J. Biol. Chem.* **270**, 6901–6907.
8. Shen, J.-R., Ikeuchi, M. & Inoue, Y. (1997) Analysis of the *psb*U gene encoding the 12 kDa extrinsic protein of photosystem II and studies on its role by deletion mutagenesis in *Synechocystis* sp. PCC 6803. *J. Biol. Chem.* **272**, 17821–17826.
9. Shen, J.-R., Qian, M., Inoue, Y. & Burnap, R.L. (1998) Functional characterization of *Synechocystis* sp. PCC 6803 *psb*U and *psb*V mutants reveals important roles of cytochrome *c*-550 in cyanobacterial oxygen evolution. *Biochemistry* **37**, 1551–1558.
10. Boekema, E.J., Hankamer, B., Nield, J. & Barber, J. (1998) Localization of the 23-kDa subunit of the oxygen-evolving complex of photosystem II by electron microscopy. *Eur. J. Biochem.* **252**, 268–276.
11. Boekema, E.J., Hankamer, B., Bald, D., Kruip, J., Nield, J., Boonstra, A.F., Barber, J. & Rögner, M. (1995) Supramolecular structure of the photosystem II complex from green plants and cyanobacteria. *Proc. Natl Acad. Sci. USA* **92**, 175–179.
12. Jansson, S. (1994) The light-harvesting chlorophyll *a*/*b*-binding proteins. *Biochim. Biophys. Acta* **1184**, 1–19.
13. Boekema, E.J. & van Roon, H., Calkoen, F., Bassi, R. & Dekker, J.P. (1999) Multiple types of association of photosystem II and its light-harvesting antenna in partially solubilized photosystem II membranes. *Biochemistry* **38**, 2223–2239.
14. Gantt, E. (1980) Structure and function of phycobilisomes: light harvesting pigment complexes in red and blue-green algae. *Int. Rev. Cyt.* **66**, 45–80.
15. Mörschel, E. & Schatz, G.H. (1987) Correlation of photosystem-II complexes with exo-plasmatic freeze-fracture particles of thylakoids of the cyanobacterium *Synechococcus* sp. *Planta* **172**, 145–154.
16. Bald, D., Kruip, J. & Rögner, M. (1996) Supramolecular architecture of cyanobacterial thylakoid membranes: how is the phycobilisome connected with the photosystems? *Photosynthesis Res.* **49**, 103–118.
17. Boekema, E.J. & van Roon, H. & Dekker, J.P. (1998) Specific association of photosystem II and light-harvesting complex II in partially solubilized photosystem II membranes. *FEBS Lett.* **424**, 95–99.
18. Kuhl, H., Krieger, A., Seidler, A., Boussac, A., Rutherford, A.W. & Rögner, M. (1998) Characterisation and functional studies on a new photosystem II preparation from the thermophilic cyanobacterium *Synechococcus elongatus*. In *Photosynthesis: Mechanisms and Effects* (Garab, G., ed.), Vol. II, pp. 1001–1004. Kluwer, Dordrecht, the Netherlands.
19. Harauz, G., Boekema, E. & van Heel, M. (1988) Statistical image analysis of electron micrographs of ribosomal subunits. *Methods Enzymol.* **164**, 35–49.
20. LeLong, C., Boekema, E.J., Kruip, J., Bottin, H., Rögner, M. & Sétif, P. (1996) Characterization of a redox active cross-linked complex between cyanobacterial photosystem I and soluble ferredoxin. *EMBO J.* **15**, 2160–2168.
21. Boekema, E.J. & Van Heel, M.G. (1989) Molecular shape of I erythrocruorin studied by electron microscopy and image processing. *Biochim. Biophys. Acta* **957**, 370–379.
22. Van Heel, M. (1987) Similarity between images. *Ultramicroscopy* **21**, 95–100.
23. Boekema, E.J. & Rögner, M. (1996) Electron microscopy. In *Biophysical Techniques in Photosynthesis* (Amesz, J. & Hoff, A.J., eds), pp. 325–335. Kluwer, Dordrecht, the Netherlands.
24. Han. K.-C., Shen, J.-R., Ikeuchi, M. & Inoue, M. (1994) Chemical crosslinking studies of extrinsic proteins in cyanobacterial photosystem II. *FEBS Lett.* **355**, 121–124.
25. Shen, J.-R. & Inoue, I. (1993) Binding and functional properties of two new extrinsic components, cytochrome *c*-550 and a 12-kDa protein, in cyanobacterial photosystem II. *Biochemistry* **32**, 1825–1832.
26. Xu, Q.A. & Bricker, T.M. (1992) Structural organization of proteins on the oxidizing side of photosystem II: two molecules of the 33 kDa manganese-stabilizing protein per reaction center. *J. Biol. Chem.* **267**, 25816–25821.
27. Betts, S.D., Ross, J.R., Pichersky, E. & Yocum, C.F. (1997) Mutation Val235Ala weakens binding of the 33-kDa manganese stabilizing protein of photosystem II to one of two sites. *Biochemistry* **36**, 4047–4053.
28. Bricker, T.M. & Frankel, L.K. (1998) The structure and function of the 33 kDa extrinsic protein of photosystem II: a critical assessment. *Photosynthesis Res.* **56**, 157–173.
29. Frank, J. (1980) The role of correlation techniques in computer image processing. In *Computer Processing of Electron Microscope Images* (Hawkes, P.W., ed.), pp. 187–222. Springer, Berlin.
30. Dekker, J.P., Boekema, E.J., Witt, H.T. & Rögner, M. (1988) Refined purification and further characterization of oxygen-evolving and Tris-treated photosystem II particles from the thermophilic Cyanobacterium *Synechococcus* sp. *Biochim. Biophys. Acta* **936**, 307–318.
31. Nilsson, F., Simpson, D.J., Jansson, C. & Andersson, B. (1992) Ultrastructural characterization of a *Synechocystis* 6803 mutant with inactivated psbA genes. *Arch. Biochem. Biophys.* **295**, 340–347.
32. Clement-Metral, J.D., Gantt, E. & Redlinger, T. (1985) A photosystem II–phycobilisome preparation from the red alga, *Porphyridium cruentum*: oxygen evolution, ultrastructure and polypeptide resolution. *Arch. Biochem. Biophys.* **238**, 10–17.
33. Ducret, A., Möller, S.A., Goldie, K.N., Hefti, A., Sidler, W.A., Zuber, H. & Engel, A. (1998) Reconstitution, characterization and mass analysis of the pentacilindrical allophycocyanin core complex from the cyanobacterium *Anabena* sp. PCC 7120. *J. Mol. Biol.* **278**, 369–388.
34. Rögner, M., Boekema, E.J. & Barber, J. (1996) How does photosystem II split water? The structural basis of efficient energy conversion. *Trends Biol. Sci.* **21**, 44–49.